




Ecological and molecular controls of metabolic activity in microbial interactions driving ecosystem-wide methane cycling

Section I. Project objectives and Background: Despite the critical biogeochemical importance of syntrophic anaerobic methanotrophy between archaea and syntrophic bacteria – a process that prevents gigatons of methane from being released to the atmosphere every year [1–4] – there are still essential details about their physiology, interactions, and ecology that are not yet understood. Our proposed multidisciplinary research on the anaerobic oxidation of methane (AOM) and associated sediment communities aims to explore these syntrophic associations at multiple scales, from molecular and intra-consortia mechanisms to the level of microbial communities and their broader environmental interactions. This will be accomplished using state-of-the-art methods in single cell ecophysiology, genetics, viral ecology, metaproteomics, analytical imaging, and computational modeling approaches. In this section, we summarize the state of knowledge regarding these research areas and articulate three main objectives to advance understanding of AOM syntrophic consortia, their broader interactions with associated microorganisms and viruses, and their collective role as a methane sink in anoxic sediments.

- Objectives**
-  I: Develop a molecular understanding of the mechanisms driving methane-fueled syntrophic interactions
 -  II: Define and functionally characterize the microbial community, including viruses, associated with methanotrophic consortia under changing environmental conditions
 -  III: Create an integrative modeling framework to explore the ecophysiology of AOM consortia and their community interactions in environmental context

I.1 Syntrophic associations between environmental ANME archaea and bacteria catalyzing anaerobic oxidization of methane: genomic clues. Geochemical observations and thermodynamic predictions suggest that methanotrophic archaea function essentially as methanogens in reverse: methanotrophy through syntrophy with sulfate-reducing bacteria [5–7], a hypothesis supported by early metagenomic observations of similarities in the canonical 7-step methanogenesis pathway between diverse ANME archaea and methanogens [8–13]. Recent evidence by our team and others indicates that the ANME methanotrophic lifestyle is not as simple as reversing methanogenesis, as it requires several modifications in energy conservation pathways and electron transfer mechanisms that are missing in methanogenic relatives [14–18]. With our recently updated library of 90 metagenome assembled genomes (MAGs) representing all major methanotrophic ANME archaea (ANME-1, Methanoperedenaceae, ANME-2a/b, ANME-2c, and ANME-3), we are developing a fuller picture of not only the genomic elements that differentiate methanotrophic archaea from methanogens, but also the features that are diagnostic for distinct ANME lineages and hypothesized to be important in their specific syntrophic associations [14].

Environmental metagenomes, Bioorthogonal Noncanonical Amino Acid Tagging (BONCAT)-based fluorescence activated cell sorting (FACS) and sequencing of single aggregates [19], and AOM enrichment cultures [20] have been used to reconstruct the genomes of diverse syntrophic bacterial partners that belong to one of four clades of the phylum Desulfobacterota: SeepSRB1a, SeepSRB1g, SeepSRB2, and *Ca. Desulfococcus auxilii* [21–24]). As with the distinct ANME lineages, these syntrophic sulfate-reducing bacteria (SRB) show clade-specific differences, pointing to potential variation in their ecophysiology and interspecies interactions with their ANME partner. Each lineage appears capable of autotrophic growth and dissimilatory sulfate reduction, but the specific respiration, bifurcation/confurcation potential, and central carbon fixation pathways differ [21–23, Murali et al., in prep]. In addition, clade-specific differences in the potential for nitrogen fixation, vitamin auxotrophy (**Fig.1A**), biofilm formation, and intercellular communication appear to be shaped by specialization with specific methanotrophic ANME – hypotheses we intend to test in the proposed work here.

Even more nuanced patterns in metabolic variation are now emerging at the level of co-existing ANME strains. Our preliminary genomic investigation of highly related ANME-2b and syntrophic partners

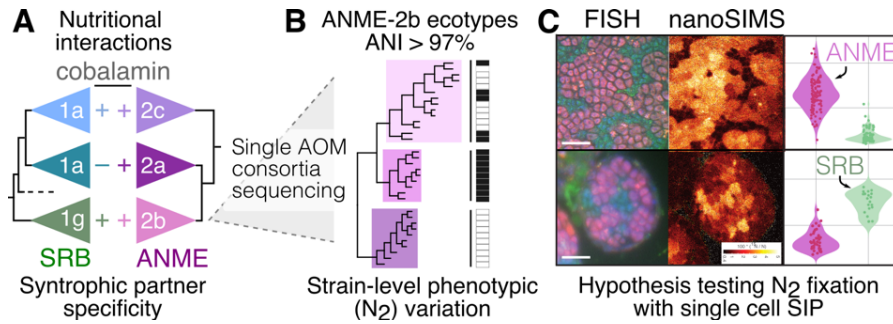


Fig 1. A) Genomic analysis of ANME-2 and their specific SRB partners indicate clade-specific variation in cobalamin auxotrophy, with a clade of SeepSRB1a (teal) lacking cobalamin biosynthesis partnering with ANME-2a to compensate for this loss (Murali et al., in prep). **B)** ANME-2b strains from single-aggregate metagenomes show differing N_2 fixation potential, suggestive of physiologically distinct co-occurring ecotypes. **C)** Variation and complementarity in diazotrophy in ANME-2b/SeepSRB1g consortia was found in $^{15}N_2$ FISH-nanoSIMS experiments where in some consortia ANME-2b were the primary diazotrophs (upper panel), while in others SRB1g were (lower panel).

(**Fig.1B**). We hypothesize that these strain-level differences may explain the physiological variation in diazotrophy among ANME-2b recently observed in our nanoSIMS single cell resolved ecophysiology experiments (**Fig.1C** [24]). These examples hint at the development of nutritional dependencies in consortia and the potential for niche differentiation among co-occurring ecotypes [25–27], an important feature that would have been missed through conventional metagenomic investigations without the ability to sequence individual consortia and accurately connect representative genomes from different subclades to their corresponding syntrophic partners. **We will leverage our unique single consortia MAGs from activity-based BONCAT-FACS to guide genetic investigations (III.1.a), culture-independent ecophysiological experiments (III.2.a), and community metabolic modeling (III.3.b) for AOM syntrophic partner pairings predicted to have distinct physiological characteristics.** Combined, this information will allow us to identify and test the underlying mechanisms shaping the co-association patterns observed among these uncultured syntrophic associations.

I.2 Manipulation of the AOM partnership: A window into syntrophic gene expression. Metagenomic-based investigations of environmental AOM syntrophy at both the single consortia and community level have been foundational for understanding patterns in interspecies partnerships and their underlying metabolic potential [10, 19, 24, 28]. To go beyond genomic inference, however, requires complementary comparative 'omics methods at the level of transcription/translation and physiological experiments. This type of comparative data for metabolically interdependent and non-syntrophic modes of growth is largely absent for uncultured microbial syntrophies like the environmental AOM consortia studied here, as methods for decoupling these relationships are often lacking. In a key development by PI Orphan's team [29], we showed the ability to manipulate the AOM syntrophic partnership, using the humic acid analog, anthraquinone 2,6-disulfonate (AQDS), as a sink for methane-sourced electrons produced by ANME. Exposure to AQDS resulted in equivalent rates of AOM and anabolic activity by the ANME in the absence of activity by the syntrophic SRB [29, 30]. This chemical manipulation strategy introduces new opportunities to target changes in physiology and expression by methanotrophic ANME archaea during syntrophic growth, or independent of an active SRB partner. Our recent comparative metatranscriptomics study of AOM sediments amended with AQDS or SO_4^{2-} as the terminal electron acceptor revealed important differences in the physiological response between two major co-occurring ANME families [30]. These experiments also contributed additional support for direct interspecies electron transfer (DIET; see reviews by [31, 32]) as the dominant syntrophic mechanism in AOM, and showed that, contrary to a previous report [33], ANME-2 do not respire sulfate, but are stimulated by it. In active syntrophic growth relative to AQDS-decoupling, ANME-2a upregulated many key genes related to methane oxidation and hypothetical DIET functions, while ANME-2c transcripts did not differ significantly, suggesting differences in their adaptation

(from co-occurring BONCAT-FACS sorted consortia [19, 24]) revealed substantial population structure within AOM sediment incubations, with distinct clusters of strains that differed by tens to hundreds of genes but shared 97% ANI and >99% 16S rRNA similarity. Distinct strain clusters appear to encode different metabolic potential, notably N_2 fixation, which was found to be differentially present across strains

and response to altered partner interactions. Surprisingly, preliminary comparative metaproteome analyses with Co-I Hettich reveal that the percentage of proteins differentially expressed by ANME during syntrophy vs. AQDS methanotrophy (16% of 1300 proteins) was higher than observed by transcriptomics, with 2-4% [34] of ~2000 total protein coding genes showing 2-fold or greater expression, suggesting regulation at the proteome level is important for these slow-growing methanotrophic consortia. **We propose to expand these comparative AQDS experiments to include new microcosm manipulation strategies that enable us to dynamically track the transition from non-syntrophic AOM by ANME to the reestablishment of SO₄-based syntrophy (III.2.a), leveraging environmental metaproteomics alongside single cell ecophysiology experiments (III.1.b,c; III.2.b) and modeling (III.3.b).** Combined, these manipulation experiments and methodologies will provide a more mechanistic understanding of syntrophic intra-consortia dynamics and niche differentiation between uncultured co-occurring ANME and SRB lineages.

I.3 Developing a genetically tractable model archaeon for anaerobic methanotrophy. Despite decades of dedicated efforts, attempts to isolate either ANME or obligately syntrophic SRB in pure culture have not succeeded. As a result, it has been difficult to parse the molecular basis of syntrophy between ANME and SRB using traditional genetic or biochemical tools. In principle, this challenge could be overcome by engineering ANME-SRB consortia *de novo*. Closely related, genetically tractable microorganisms could be used as a genetic chassis for each partner, and relevant genes can be introduced in the appropriate host background to recreate and characterize a synthetic ANME-SRB consortium in a laboratory setting. There are several well developed genetic systems in related model bacteria for expression of syntrophic partner genes (e.g. *Geobacter*) we have begun to work with [34, Jiménez Otero and Murali, in prep], which will be available for co-culture experiments (III.1.a); however, our primary focus here will be to incorporate the latest genetic tools for studying ANME archaea. Methanogenic archaea belonging to the genus *Methanosarcina* are especially well-suited to serve as a heterologous host for expressing and studying ecologically important genes from ANME. First, *Methanosarcina* spp. are closely related to many ANME, in particular the most recently evolved ANME-3 methanotrophs nested within the family Methanosarcinaceae [14]. Next, these two groups of microorganisms share a large repertoire of core metabolic genes involved in carbon transformation and energy conservation during methane metabolism; thus, only genes predicted to have a specific role in symbiosis would need to be imported into *Methanosarcina* spp. Third, unlike many other genetically tractable archaea that grow under extreme conditions, *Methanosarcina* spp. are mesophilic, with optimal growth conditions (e.g. T, pH, salinity) similar to those observed for many ANME-SRB consortia. Thus, any proteins derived from ANME should be able to fold and function properly in *Methanosarcina* spp. Finally, and importantly, a broad collection of genetic tools for mutagenesis and chromosomal manipulation of *Methanosarcina* spp. can be harnessed for tunable expression and functional analyses of individual genes or pathways derived from ANME. Notably, the recent development of CRISPR-Cas9 genome editing tools by Co-I Nayak have tremendously improved the scale and scope of genetic analyses that can be performed with *Methanosarcina* spp. [35]. **With the incorporation of this model archaeon and state-of-the-art CRISPR-cas9 gene editing by Co-I Nayak, we now have the tools to go beyond comparative gene expression and genomic inference to direct characterization of promising gene targets, including those currently lacking annotations, which we hypothesize are important to AOM syntrophy (III.1.a).**

I.4 Expanding the microbial interaction sphere connected to syntrophic AOM. Although our central focus has been on ANME-SRB interactions, these consortia do not exist in isolation. Rather, they interact with a diverse microbial and viral community which impact the consortia themselves and, potentially, the rates and spatial extent of AOM. Most environmental AOM consortia reported from FISH microscopy studies occur as two-member consortia or larger aggregations of the same ANME-SRB type ([16, 36–39]; Fig.2). However, our recent microscopy surveys, single consortia metagenomic sequencing (BONCAT-FACS) from methane-rich sediments, and reports from sulfate-coupled AOM enrichments [28, 40] have painted a more complex picture, with members of multiple ANME lineages and SRB co-occurring together with non-ANME/SRB members (Fig.2 C, D). Additionally, we have now successfully propagated five sediment-free anaerobic AOM enrichments dominated by large aggregations of methane-oxidizing ANME-

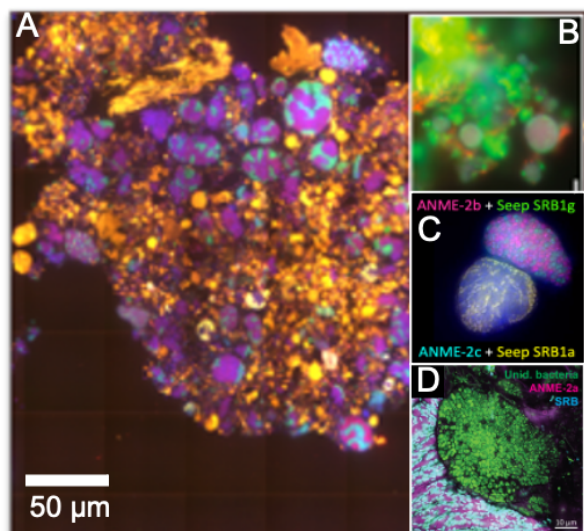


Fig.2. FISH images of ANME-SRB consortia in lab incubations. **A)** Sectioned sediment with numerous ANME (pink) and SRB (teal) consortia. Sediment particles are orange. **B)** AOM aggregates (ANME-2a, in red, SRB green) in thick EPS matrix (green autofl) from sediment-free AOM enrichment. Scale 10µm. **C)** physical association and as yet unknown ecological interactions between two different ANME-SRB consortia types. **D)** Unidentified bacteria (green) in physical association with ANME-SRB (red & cyan).

2a/2b with SeepSRB1a and SeepSRB1g (**Fig.2B**), along with several bacterial groups (e.g. Anaerolineae, Bacteroidales, and Patescibacteria) and methanogens affiliated with the *Methanococcoides* [20]. The co-occurrence of methylotrophic methanogens (non-SRB bacteria) observed by our team and others [19, 20, 28, 41, 42] suggests the potential for local methane cycling and expanded metabolic interactions [43–47]. FACS sorting and sequencing of individual aggregates from our enrichments indicate that these methanogens occur in physical association with ANME and SRB and contain genes required for methylamine and methanol-based methanogenesis, a feature absent from ANME [20]. The source of the methylated substrates fueling these persistent associations in the AOM enrichments – whether produced by ANME “spillover” reactions [28] or other co-occurring microorganisms – is currently unknown. **Addressing potential underlying metabolic interactions between these and other co-occurring methanogenic and methanotrophic archaea, along with several of the putative heterotrophic bacterial MAGs recovered from AOM aggregates, will be a focus of incubation and transparent soil experiments (III.2.a; III.3.a) coupled with community-level metabolic modeling, CMM (III.3b), expanding the**

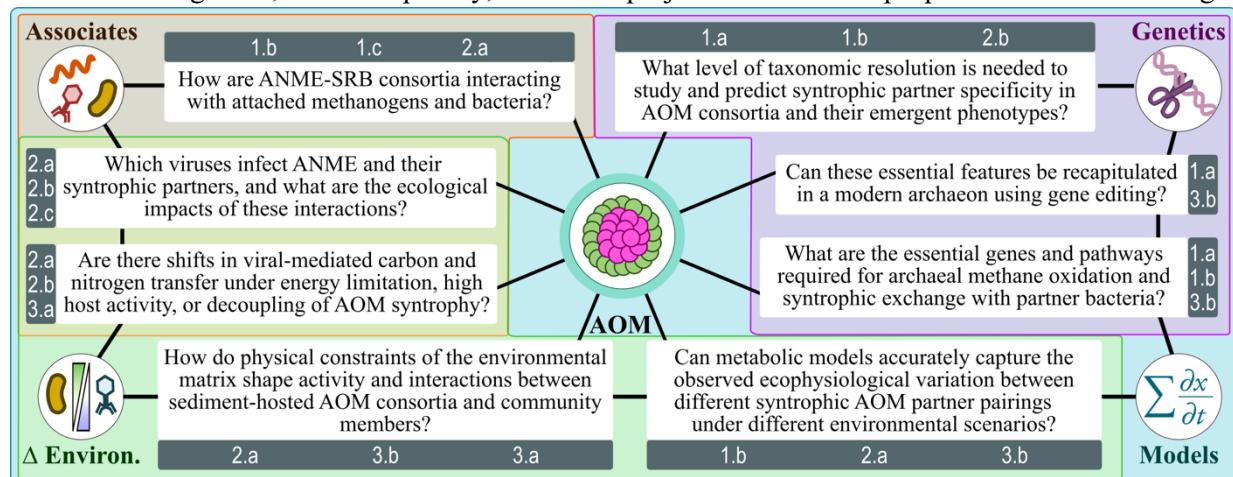
network of microorganisms interacting with AOM consortia.

I.5 Viruses associated with AOM systems: state of knowledge and methods development. Like associated bacteria and archaea, viruses, numbering in the billions per gram of methane-rich sediment, form part of the expanded AOM consortia interactions sphere. Recent studies have indicated a role for viruses in methane cycling in soils [48–50]; however, our knowledge of potential interactions between viruses and syntrophic consortia in methane-saturated sediments, and the impact on their activity and biogeochemical transformations, has been limited [51–53]. Through our current DOE-supported research, metaviromic analysis of viral concentrates from our AOM sediment incubations yielded 3,400 complete viral metagenome-assembled genomes (vMAGs). The majority of vMAGs are currently unclassified; however, several head-tail Siphoviruses and Haloviruses have been identified [**Philosof et al., in prep**]. Parallel TEM analyses of viral morphology confirmed the presence of spindle-shaped halovirus-like particles, tailed Caudoviricetes, and several novel morphologies (**Fig.6**). Notably, CRISPR spacer matching with several of our near-complete ANME-1 genomes uncovered a remarkable diversity of dsDNA viruses that may infect ANME-1, including head-tail Caudoviricetes, Varidnaviria, Adnaviria, and multiple spindle-shaped viruses [**Perez-Laso, Wu et al., in prep**]. Several of the recovered vMAGs also contained Auxiliary Metabolic Genes (AMGs; [54]), including genes involved in heme biosynthesis, assimilatory sulfate reduction, amino acid recycling, and carbohydrate metabolism. **The metagenomic insights into the AMGs encoded by viruses in our AOM sediment incubations and their potential hosts provide the backdrop for more detailed activity-based analyses, where we will characterize environmental viral populations using stable isotope probing experiments with viral-nanoSIMS [55], Protein-SIP (III.2.b), and viral BONCAT-FACS (III.2.c), and incorporate them into models (III.3.a,b).** This will expand our ecological understanding of viral interactions with diverse syntrophic AOM consortia, factors impacting viral production rates, and their impact on geochemical transformations of CH₄, S, and N in sediments.

I.6 Analytical imaging of spatial dynamics in structured syntrophic consortia. To complement our meta’omics results (above), we have developed and optimized several synergistic methodological strategies that allow for direct analysis of activity and ultrastructure of environmental syntrophic consortia, single microbial cells, and viruses in sediments. These include analytical imaging modalities, including fluorescence (BONCAT, HCR-FISH, and seqFISH), X-ray (XRF), electron (serial block face, and secondary ion (nanoSIMS) [16, 24, 29, 30, 56, 57]; Fig.1C). For example, single-cell mRNA detection using sequential FISH (seqFISH, [58, 59]) and hybridization chain reaction FISH (HCR-FISH [60]) have been recently optimized for visualizing expression of individual genes (e.g. *nifH*, *mcrA*, and the putative electron conduit, *oetL*) in environmental AOM consortia, ([24]; Fig.4). **Multiplexing of multiple mRNA targets coupled directly with single cell stable isotope probing by nanoSIMS (and, where relevant, chemical imaging with XAS) will be an objective of our work here, providing the ability to visualize the expression of key genes and directly compare with cell-specific metabolic activity while maintaining spatial context (III.1.b, III.2.b).**

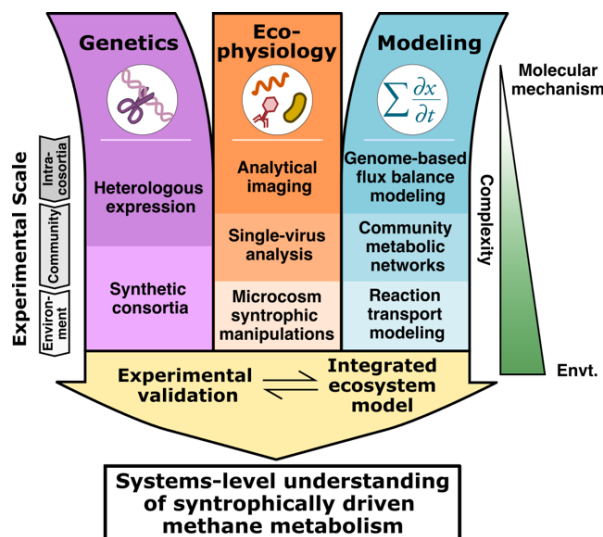
Essential evidence supporting direct interspecies electron transfer (DIET) as the likely syntrophic mechanism driving sulfate-coupled AOM was developed not simply through genetic inference (e.g. genes encoding large multiheme cytochromes), but also from complementary analytical imaging methods and reaction-transport modeling of AOM consortia [9, 14, 16, 17, 22]. The use of electron-microscopy-compatible heme stains with Co-I Ellisman revealed extracellular localization of MHC proteins hypothesized to be used for direct electron transfer between syntrophic ANME and SRB partners [16]. Additionally, optimization of single cell resolved FISH-nanoSIMS stable isotope-based measurements of anabolic activity in environmental ANME-SRB consortia revealed patterns of cellular activity and spatial distance between syntrophic partners that were inconsistent with thermodynamic constraints and reaction-transport models (Co-I Meile) of common diffusible syntrophic intermediates like H_2 [6, 61–63], and better fit models of direct interspecies electron transfer [16, 62, 64]. EM imaging and 3D reconstruction of AOM consortia using serial block face imaging and tomography ([56]; Co-I Ellisman) has also provided novel insights (e.g. outer membrane vesicles, OMV, which may be involved in cell-cell communication [65–68] Fig.5), and introduced new questions about ANME-SRB ultrastructure and interactions that were not readily apparent through ’omics methods alone. **Given the recognized importance of DIET in ANME-SRB syntrophy, examining the composition and structure of the extracellular matrix – the space in which electron exchange and cell-cell interactions occurs – is a critical next step, and one that we are well positioned to accomplish.**

II. Motivating questions: Our goals for this proposal are to develop a mechanistic framework for understanding the fundamental components of cooperative anaerobic methanotrophy between ANME archaea and syntrophic partner Desulfobacteraceae bacteria, and to define the nature of interactions occurring with other associated microbes and viruses in the context of conditions in the local sediment matrix. This integrative, multidisciplinary, multiscale project aims to develop a predictive understanding of



the complex network of microbial interactions shaping methane cycling in anoxic sediments. Our experimental approach will address our three main objectives described above, organized around several motivating questions highlighted in the figure above (with subsections of **III** listed in gray bar for each).

III. Experimental approach: The multidisciplinary research team assembled here synergistically merges expertise and state-of-the-art, culture-independent analytical methods, combining experimental (**ecophysiology**, viral ecology, **genetics**, metaproteomics, analytical imaging) and computational **modeling** approaches (genome-based metabolic modeling of microbial communities and reaction transport simulations). We will strategically employ these approaches in various permutations to address the motivating questions outlined above, collectively working towards developing an in-depth, systems-level understanding of the interactions and specific molecular mechanisms that contribute to the structure, stability, and biogeochemical activities of anaerobic microbial communities in methane-rich sediments. **Below we describe our experimental approach, which combines bottom-up reductionist (molecular, cellular) and top-down community-level (ecological interactions) methods using currently established techniques by the Co-I's alongside new methodological strategies categorized as high-risk, high-reward for our project goals and relevant to DOE's Genomic Science objectives.**



III.1.a Leveraging genetics and synthetic consortia (CRISPR-Cas gene editing in *Methanosarcina*): Towards a mechanistic molecular understanding of AOM syntrophy. Genetic tools have been used to uncover mechanistic information about relationships between syntrophic partners, but this approach is currently constrained to a subset of microorganisms in culture. Nonetheless, the power of genetics can still be leveraged in the study of uncultured microorganisms and syntrophic associations using heterologous expression in related genetically tractable microbial hosts. In the context of the uncultured methanotrophic ANME archaea, Co-I Nayak has recently pioneered CRISPR-Cas9 genome-editing tools in methanogenic archaea [35, 69], enabling rapid and efficient genetic manipulation of *Methanosarcina acetivorans*, an archaeon closely related to members of ANME-2 and ANME-3 [14]. CRISPR-Cas9 offers several advantages over other genetic techniques in *M. acetivorans*, including 3-4x decrease in time for production of scarless mutant strains, and enhanced capability to simultaneously introduce multiple mutations (up to 6), which can range from single SNP's to large >1kb indels, and chromosomal inversions. Here we propose to apply Nayak's state-of-the-art gene editing in *M. acetivorans* as a laboratory model system to 1) characterize the function of target ANME genes and their phenotype in *Methanosarcina* mutants and 2) develop model synthetic consortia using modified *Methanosarcina* and either native electrogenic sulfate-reducing microorganisms (e.g. *Desulfuromonas* [70]) or the genetically tractable electrogenic model organism *Geobacter sulfurreducens* [34, 71, 72]. These mutants and synthetic consortia will enable direct testing of genes predicted to be involved in partner recognition and interspecies syntrophic interactions, including expressed genes that are currently not well annotated that are unique to methanotrophic ANME.

In a collaborative pilot study between Nayak and Orphan, CRISPR-Cas9 technology was recently used to express and characterize components of the unique ANME-2/3 membrane complex (McoAB) with a putative role in extracellular electron transport (EET) in *M. acetivorans* [Gupta et al., in prep]. These initial findings indicate that CRISPR-Cas9 gene editing can be used to not only introduce novel functionality but also alter core metabolic pathways in *Methanosarcina*. Complementary genetic analyses for syntrophic SRB partners are also being tested in *Geobacter sulfurreducens* in collaboration with

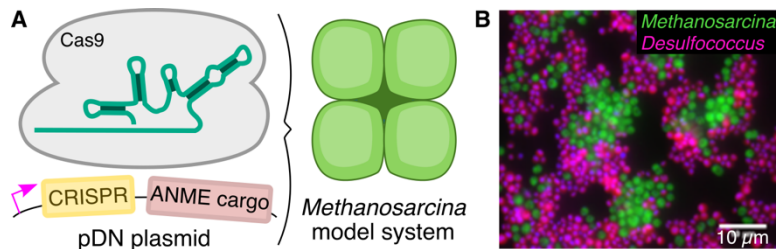


Fig. 3. Genetic manipulation of *Methanosarcina* for the heterologous expression of ANME proteins. A) CRISPR-Cas9 gene editing will be used to introduce ANME genes predicted to be involved in energy conservation and syntrophic partnership formation with SRB into the archaeal model system. B) Example of aggregated co-culture of *Methanosarcina* (green) and SRB (here *Desulfococcus*; magenta) as a model to experimentally test genetic elements of ANME syntrophy.

mechanisms predicted in the genomes of ANME archaea. Building from our recent comparative analysis of ANME genomes, including the most recently evolved methanotrophic ANME-3 lineage within the family Methanosarcinaceae, has enabled the identification of several genes and pathways which we hypothesize are essential for methanotrophic growth and establishing syntrophic partnerships with specific lineages of bacteria (**Fig.5c**; [14]). Our analysis of ANME-3 genomes, for example, indicates the modification of several genes that are common or unique to ANME, including modifications of genes in central metabolism, and several genes potentially involved in partner interactions, e.g. phage-like protein translocation systems, or PLTS, a Type VI-like contractile injection system conserved in all ANME lineages [14]. Preliminary proteomics analysis (Co-I Hettich) indicates that the expression of this system is depressed under conditions where the syntrophic association was disrupted with AQDS. Our combined application of genetics with high-resolution structural analyses (EM and cryo-EM) of both native AOM consortia and *Methanosarcina* mutants expressing PLTS will be used to characterize these structures and understand their role in ANME (**III.1.c**).

III.1.b Intra-consortia scale: Differentiating ecotypes and visualizing expression patterns with single cell spatial transcriptomics – HCR and seqFISH. Caltech colleague L. Cai is a pioneer in the development of spatial transcriptomics techniques; as part of our currently funded DOE, we have optimized sample handling, seqFISH probe design, and hybridization conditions for uncultured sediment-hosted consortia (**Fig.4**). Now, informed by our genomic analyses and metatranscriptomics data, we will employ seqFISH to examine spatial patterns in gene expression for distinct ANME and syntrophic bacterial partner pairings and between co-occurring strains. Examples of initial targets include formate dehydrogenase (hypothesized to be involved in AOM syntrophy [63]), *omcS/X* linked to EET in SRB partners [**Murali et al., in prep**], *napH*, *mcoAB*, and *rnf* in ANME [14], and genes connected to interactions in the extracellular matrix (ECM; biofilm formation *pel/pilY1*; proteins with cohesion-dockerin domains; archaellum; and PLTS injection systems, targets that will also be used for genetic characterization with Co-I Nayak (**Fig.5**)). In-house seqFISH experiments with 1-2 target genes have recently been optimized; however, multiplexing with multiple probes is best accomplished with an automated platform that directly combines confocal imaging with automated liquid handling, enabling multiple rounds of hybridization/dehybridization on the same target [59]. This custom imaging system, developed by Cai, will enable us to significantly scale up the number of mRNA targets across multiple AOM consortia types recovered from microcosm experiments (letter Glasser). Importantly, our environmental sample processing pipeline and embedding resin for sediment AOM consortia is compatible with both fluorescence mRNA detection by seqFISH and single cell stable isotope analysis by nanoSIMS, allowing direct correlation of microbial identity and gene expression with metabolic activity and phenotypic variation within and between AOM consortia recovered at different time points from our incubation experiments. Similar multi-probe fluorescent labeling strategies will also be applied with the goal of differentiating closely related strains or ecotypes of co-occurring

Fernanda Jiménez-Otero (Naval Research Laboratory), where heterologous expression using RK2 vectors that utilize a native promoter [73] were used to introduce multiheme cytochromes common to the syntrophic SeepSRB partners of ANME in a *G. sulfurreducens* mutant, and shown to rescue electrogenic activity [**Jiménez-Otero and Murali, in prep**]. These *Geobacter* mutants will be available for reconstructing synthetic consortia with various *M. acetivorans* mutants expressing key energetic and syntrophy-enhancing

ANME-2 (and SRB) in our incubation experiments and will be used in combination with nanoSIMS experiments to determine differences in their ecophysiology in microcosm experiments. Assessing the specificity of FISH probes for environmental microbes is often challenging, but can be overcome using a similar serial hybridization strategy, where multiple rounds of hybridization are conducted on the same resin embedded target, enabling direct testing of specificity with multiple probe combinations and optimization of hybridization conditions. Multiplexing tens to hundreds of gene targets in complex environmental communities with seqFISH+ [59, 74] is an important next step in the progression of spatial transcriptomics and will enable us to map the expression of genes and pathways hypothesized to be important in energy conservation and interactions within the spatial context of syntrophic partnership [16, 62].

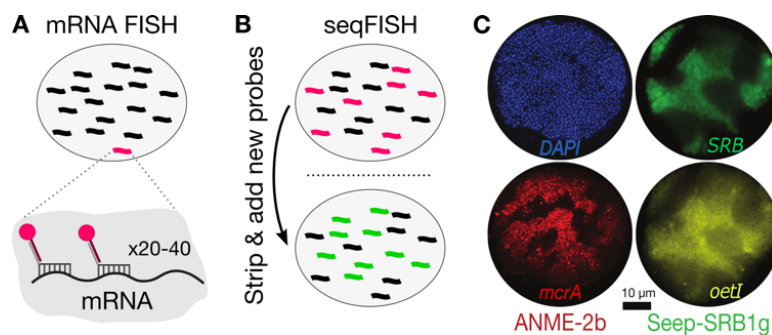


Fig 4. Progress towards developing single cell transcriptomics in environmental ANME-SRB consortia. **A / B**) schematic of SeqFISH protocol for single cell mRNA visualization, compatible with multiplexing numerous gene targets through successive hybridization/dehybridization with different probe combinations **C**) Expression of mRNA targets in thin sectioned samples of two different environmental AOM consortia, including the highly expressed *mcrA* in ANME-2 (red) detected with SeqFISH, counterstained with DAPI (blue) and the hypothesized extracellular electron transfer conduit *oetI* (yellow) in the ANME-2b syntrophic partner Seep-SRB1g detected with HCR-FISH amplification described in [24]. SRB partner identity was determined by 16S rRNA FISH (green).

III.1.c Intra-consortia scale: Ultrastructural characterization of cell-cell interactions, EM approaches. The inherently organized multicellular structure of AOM consortia and evidence of direct extracellular electron transfer between ANME and their syntrophic SRB partners spotlights the importance of gaining a deeper understanding of the molecular composition, fine structure, and interspecies interaction mechanisms of the extracellular matrix (ECM). Co-I's Ellisman and Orphan have optimized several sample processing and advanced EM imaging techniques that are compatible with other analytical imaging modalities, including X-ray (XAS) and nanoSIMS. This has helped to resolve unique ultrastructural features – including poly P, carbon storage granules, and magnetosome-like FeS chains – that vary among environmental AOM consortia [23, 56, 75]. We will apply EM-based imaging to characterize membrane-associated and extracellular features detected in ANME and SRB genomes, which we hypothesize play a role in syntrophic partner recognition and interactions within consortia. Using a combination of light and EM compatible stains (e.g. DRAQ5 for eDNA, lectin staining of glycoconjugates [76–78], and lipid stains (FM4-64; [78]), we will prepare and analyze AOM consortia from our experimental incubations after stable isotope or HPG labeling for BONCAT (**III.2.a**; [19]). Comparison between incubation conditions will allow us to assess how ECM components (e.g. outer membrane vesicles; **Fig.5B**) change in response to deactivation/reactivation of the SRB syntrophic partner (e.g. transition from AQDS growth condition back to sulfate) or under conditions where the electron donor/acceptor is limiting. Examples of the ECM associated targets for both ANME and SRB are highlighted in **Fig.5C**. Sample processing for multi-modal TEM imaging and nanoSIMS analysis with Co-I Ellisman at NCMIR will include the transfer of parallel thin sections onto conductive silicon wafers for nanoSIMS analysis [56, 63], where, by enhancing the nanoSIMS spatial resolution, we will quantify the transfer of isotopically labeled organic nitrogen and sulfur compounds into the ECM surrounding active and inactive ANME and SRB cells (see preliminary results in **Fig.5E**). Additionally, the upregulation of PLTS contractile injection systems in ANME during syntrophic growth (**III.1.a**) suggests that these molecular machines play a role in structuring interactions within consortia. In collaboration with M. Pilhofer, a leading expert in cryotomography of contractile

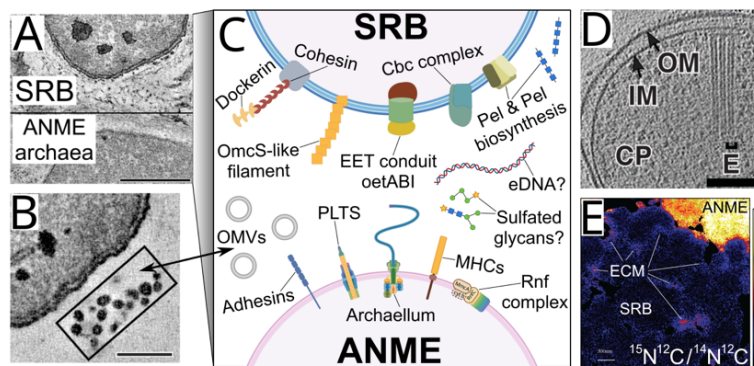


Fig. 5 **A)** TEM image of an environmental ANME-SRB aggregate showing fine-scale structure in the extracellular matrix (ECM) and carbon-rich granules in the SRB **B)** Close-up of an SRB cell from this consortium revealing inner-membrane invaginations and a cluster of outer membrane vesicles (OMV, ~50 nm diameter). OMVs were commonly observed to be distributed within consortia, but clusters shown here were rare, scale= 200 nm (from [68]). **C)** Cartoon showing several candidate membrane-associated and ECM components conserved in ANME and SRB genomes that are predicted to be involved in partner recognition/ communication within syntrophic AOM consortia that will be investigated in this proposal. **D)** Cryotomography of a Type VI like contractile injection system ‘e’ in a symbiotic bacterium from collaborator M. Pilhofer, scale=100nm [79] structurally similar to the predicted phage-like protein translocation structure (PLTS) in ANME. **E)** nanoSIMS ion image of cells in AOM consortia from an AQDS sediment incubation amended with $^{15}\text{NH}_4$ showing ^{15}N enrichment in the ECM surrounding inactive SRB cells (arrows), adjacent to an active ANME suggestive of active excretion and transport of an ANME-sourced N-containing macromolecule in the matrix surrounding ANME and SRB.

(exchange with $\text{N}_2:\text{CO}_2$ mix). Consortia positions will be registered, and these samples will be immediately processed in the chamber by freeze substitution, enabled by the new Leica imaging pipeline at NCMIR. With this multi-modal imaging strategy, we can specifically target consortia exhibiting variations in cellular activities during this transition period and relate this to EM resolved ultrastructure. Additionally, this cryo-sectioned material will be used for single cell transcriptomics at Caltech (seqFISH; **III.1.b**).

III.2.a Community scale: Ecophysiological interactions between ANME-SRB, associated microbes, and viruses – Syntrophic manipulation experiments. Our proposed research on AOM syntrophic assemblages is based on a collection of large (1L) 10 °C anoxic methane sediment incubations and several sediment-free AOM enrichments currently maintained at Caltech [20]. These incubations stably sustain high rates of sulfate-coupled AOM and have been well characterized using a combination of bulk metagenomics [14, 22], single consortia BONCAT-FACS sequencing [20, 24], and metaviromic analysis [Philosof et al., in prep]. We plan to build from this rich ‘omics dataset for our ecophysiology and metaproteomic experiments, analytical imaging investigations, and metabolic modeling efforts proposed here. Each of these large-scale AOM incubations supports different proportions of slow-growing methanotrophic ANME (e.g. ANME-2a, ANME-2b, ANME-2c, ANME-1) and their syntrophic bacterial partners (SeepSRB1a, SeepSRB1g, SeepSRB2, and *Ca. Desulfofervidus*), often with one consortial type dominating. Additionally, we have successfully propagated sediment-free AOM enrichments that are dominated by ANME-2a/-2b (multiple strains) and SeepSRB1a (**Fig.2B**), with several of these incubations also supporting methylotrophic methanogens (*Methanococcoides* sp.) and several uncultured putative heterotrophic bacterial lineages (**I.4**; [20]). Experiments with these sediment-free, lower-complexity

injection systems, we will structurally characterize the ANME PLTS in consortia, assessing whether these systems are membrane-bound or released into the ECM (**Fig.5D**; [79]).

The ability to conduct live cell staining and real-time observation coupled with downstream EM analysis has been previously inaccessible for investigations of AOM consortia. With the availability of sediment-free enrichments of AOM consortia (**III.2.a**) and advancements in portable environmental sample chamber design with gas exchange capabilities (e.g. CH_4 , SampLink, Leica), we now have a valuable new opportunity to conduct live confocal microscopy experiments with AOM enrichments, coupled directly with co-registered sample preparation for EM microscopy using high-pressure freezing-freeze-substitution in the NCMIR facility. Short-term incubation experiments with our AOM enrichments will be set up at Caltech and transported to NCMIR, where we will use combinations of pH-sensitive dyes and reversible cell viability stains (CTC) to track the change in cellular activity from CH_4 replete to limited conditions

enrichments offer new opportunities for live cell manipulation and ultrastructural imaging (Co-I Ellisman and collaborator Pilhofer; **III.1.c**). Transparent sediment microcosms – which retain the structure of sediments but vastly expand our ability to visualize the spatial distribution of porewater chemicals – will provide a foundation for our expanded metabolic modeling of AOM syntrophy and interactions with methanogens and other physically associated community members (**III.3.b**).

These enrichments will be used to empirically test for ecophysiological variation between co-existing ANME-2 strains and for syntrophic interactions between ANME and SRB and between methanotrophs, methanogens, and co-associated bacteria using single-cell fluorescence gene and mRNA-targeted imaging (using seqFISH and HCR-FISH; **Fig 4**; **III.1.b**) and stable isotope probing with FISH-nanoSIMS (**III.2.b**) that can be directly combined with other compatible chemical imaging (XAS; letter Webb). With doubling times of ~3 months, the AOM biomass in these enrichments may not be sufficient for replicated proteomics experiments. If found to be limiting, we will use transcriptomics data following protocols outlined in [30] to inform community modeling. These sediment-free AOM enrichments will additionally be used to inoculate custom synthesized transparent sediment matrices (**III.3.a**; [80]), providing an opportunity to use fluorescence microscopy methods and indicator dyes to examine the effect of simulated sediment pore space and permeability on cellular activity and geochemical gradients and to compare this with reaction transport models (Co-I Meile; **III.3.b**).

To expand our understanding of the spectrum of physiological interactions between different syntrophic ANME-SRB partner pairings and ecological factors influencing diverse co-existing AOM consortia in sediments, including interactions with other microorganisms and viruses, we will conduct manipulation experiments with subsampled material from our large-scale AOM sediment incubations (**III.2.a**). Replicated time course experiments, coupled with stable isotope probing (FISH-nanoSIMS) and proteomics, will be conducted under conditions of electron acceptor or donor limitation (e.g. sulfate and methane) to examine physiological differences between ANME-2c, -2a, -2b and ANME-1 consortia. Incubation conditions supporting nitrogen fixation ($^{15}\text{N}_2$) vs ammonia ($^{15}\text{NH}_4^+$) will be used to test physiological differences between *strains* of ANME-2b with and without nitrogenase (**I.1**; **Fig.1 B, C**). These experiments will additionally integrate proteomics methods (protein-SIP) with Co-I Hettich to examine patterns in expressed proteins unique to individual ecotypes and will incorporate new gene-based seqFISH protocols to fluorescently identify these unique strains (**III.1.b**), alongside our recently established single cell mRNA seqFISH/HCR-FISH protocols for ANME-SRB consortia [24].

We will also leverage our ability to experimentally decouple ANME methanotrophs from their syntrophic SRB partners through AQDS amendment [29, 30] and expand this to new experiments where we will track the molecular, ecophysiological, and ultrastructural changes that occur during the early stages of **reestablishment of syntrophy** between ANME-SRB through replacement of AQDS with SO_4 . Our latest trial experiment indicates that the suppression of the SRB partner by AQDS is reversible, with active sulfide production and SRB anabolic activity recovered after complete AQDS removal and replacement with SO_4 . This new opportunity to dynamically manipulate the syntrophic coupling between ANME and SRB through experimental cycling of AQDS and SO_4 amendments provides an unprecedented experimental framework for studying the dynamics within AOM syntrophic partnership and among other microbes and viruses interacting with AOM consortia in sediments. These manipulation experiments will be used to track changes in the metaproteome (Co-I Hettich) alongside HPG addition for BONCAT or Protein-SIP with either $^{15}\text{NH}_4^+$ or $^{18}\text{O}\text{-H}_2\text{O}$ (using MetaProSIP software at ORNL; [81–83]) and with seqFISH and FISH-nanoSIMS (using combinations of ^{13}C , ^{15}N , ^{34}S , ^{18}O -labeled substrates; also see [84]). Together these datasets provide synergistic information at both the community level and at the level of single cells and viruses, enabling us to dynamically track temporal changes in transcriptomic and metabolic activity and extracellular matrix remodeling (**III.1.c**; Co-I Ellisman), viral identity and production (**III.2.b**; Co-I Martinez-Garcia), and response by other associated community members

III.2.b Community scale: Ecophysiology of active microbial cells and viruses – nanoSIMS and BONCAT. Secondary ion mass spectrometry (SIMS and nanoSIMS) is a high-precision method for quantifying elements and stable isotopes at submicron spatial scales [85, 86]. The combination of

nanoSIMS with fluorescence microscopy and other non-destructive imaging have been powerful tools in microbial ecology for characterizing the activities of individual microorganisms [87–89] and, more recently, viruses [55] recovered directly from environmental samples. The Orphan lab has optimized sediment sample processing and single cell resolved nanoSIMS stable isotope imaging of AOM consortia after FISH labeling, using the seven independent detectors on the Caltech CAMECA nanoSIMS 50L for simultaneous quantitative analysis of ^{13}C , ^{15}N , and D/H (or ^{34}S , ^{18}O) in cells, extracellular matrix (ECM; Fig.5E), and metabolic products [16, 90–92]. While this is a destructive sampling method, nanoSIMS can be directly coupled with other complementary imaging modalities including fluorescence, electron, and X-ray spectroscopy techniques, providing information about cellular ultrastructure (electron microscopy), taxonomic identity and gene expression (FISH, seqFISH), and chemical speciation (XAS; letter Webb). The ^{13}C and ^{15}N isotopic analysis of viruses, with a size range at the limit of nanoSIMS detection (50nm), has proven more challenging. We previously demonstrated the analytical feasibility of measuring ^{13}C and ^{15}N enrichment in individual phage particles in SIP experiments with co-cultures of microbial hosts and infecting viruses [55]. However, advancing this technique to the analysis of sediment-hosted viruses required substantial redesign of our approach (Fig.6C), as native fluorescence from residual sediment particles and viral loss during washing steps precluded robust co-registration of fluorescently stained viruses with corresponding nanoSIMS ^{15}N and ^{13}C measurements. With these optimized methods, we will apply viral-nanoSIMS to our SIP microcosm experiments described in III.2.a, following the trophic transfer of nitrogen (N_2 , NH_4^+) and carbon (CO_2 , CH_4 , methanol, formate) into viruses after lysis of metabolically active host cells. Comparative experiments will be conducted under conditions of electron donor/acceptor limitation (hypothesized to alter viral productivity), after stimulating co-occurring methylotrophic methanogens and upon reactivation of ANME-SRB syntrophy.

III.2.c Community scale: Genomic and proteomic characterization of actively produced nanoscale mobile elements, FAC sorting of viruses and vesicles. Viruses interact and shape every cell in aquatic and sediment environments; therefore, unveiling the identity and impact of active viruses is paramount to provide insights into the role of these abundant biological nanoparticles in the control of AOM

consortia. Our recent metaviromic analysis of AOM sediments has provided an important foundation for understanding viral diversity and potential host interactions, which can now be complemented with new tools for single-virus genomics (SVG) using FACS sorting and sequencing ([93–95]; Co-I Martinez-Garcia), together providing a more comprehensive view of microdiversity within methane-based ecosystems. In principle, SVG can be combined with activity-based fluorescence assays (viral-BONCAT, developed by PI Orphan) for quantification and sequencing of newly produced environmental viruses [55]. In our current DOE collaboration, Co-I Martinez-Garcia optimized the viral-BONCAT protocol to maximize the signal-to-noise ratio, which was determined to be critical for FACS sorting of BONCAT-labelled viruses from the environment; however, the detection and sorting in environmental samples remains challenging. A new generation of spectral flow cytometer sorters, BigFoot, is now available at

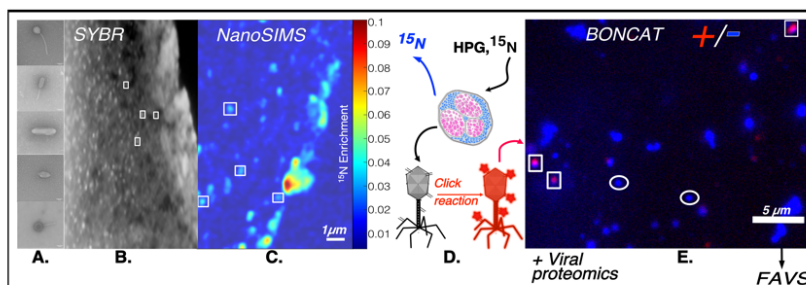


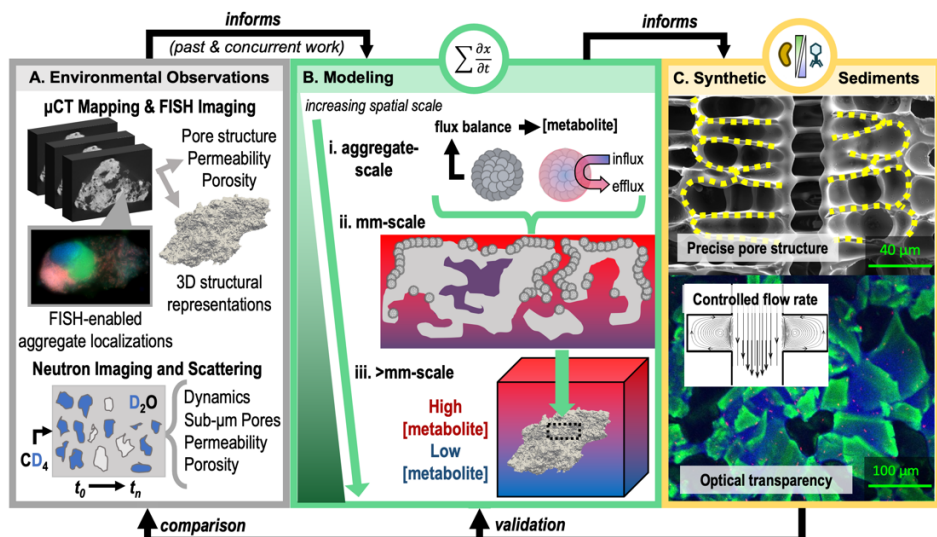
Fig. 6 Activity tracer methods for environmental viruses with nanoSIMS and BONCAT. **A)** TEM images of morphologically diverse viruses from AOM sediment incubations (50nm scale). **B)** Optimized viral-nanoSIMS protocol with ~50nm P1 phage, improving co-registration between SYBR and nanoSIMS images. Viral concentrates were first embedded in resin, sectioned, and stained with SYBR gold, followed by **C)** nanoSIMS analysis of isotopic enrichment (e.g. ^{15}N) of individual SYBR stained viruses. Correlated viral particles in SYBR and nanoSIMS are highlighted in boxes. **D)** Viral-BONCAT fluorescently tags newly produced viruses via Cu-catalyzed click chemistry. BONCAT positive (red) and negative (blue, SYBR) viruses from an AOM sediment incubation. BONCAT + and - viruses will be sorted by flow cytometry (Fluor. Activated Viral Sort.; FAVS) for single-virus genomics (SVG).

Barcelona University and Biomedical Park PRBB (Barcelona, Spain) and will be incorporated in these experiments, increasing the sensitivity and potential detection of BONCAT-labelled viruses. This will also be expanded for detection and sorting of outer membrane vesicles (OMV) using fluorescent membrane dyes (e.g. Fm4-64 or PKH26; [96]). These virus-sized lipid-bilayer spheres are released by cells and often carry genetic material, proteins, and metabolites [97–99]. The recent observation of OMV in AOM consortia (**Fig.5B**; [68]) make these a high-priority target for characterization. We will continue to develop these state-of-the-art, yet unproven sorting methods for characterizing newly produced mobile elements and, in parallel, we will also use well-vetted, lower-risk protocols for generating single viral genomes (SVG) with conventional SYBR staining and sorting of viruses from our sediment microcosm experiments (**III.2.a**). Coupled with our proposed AOM incubation experiments, we will sort and sequence 384 viruses using conventional SYBR Gold staining to establish a database of SVG. This will be followed by optimization by the BigFoot sorter for sorting BONCAT-labeled single viral particles clicked with AF647 dye. We recently observed a decrease in our ability to detect viral-like particles by flow cytometry after dual labelling (SYBR Gold and BONCAT), and believe we are likely to have greater success by sorting in one channel. To complement these assays, we will also assess the ability to detect and sort outer membrane vesicles in our microcosm experiments using the Fm4-64 dye. These assays will be tested with the FACS Aria Fusion, Influx (Barcelona) and the Sony SY3200 cell sorter at Caltech, which was recently shown to be capable of detecting BONCAT-labeled P1 phage. Sorted viral particles (or OMV) will be subjected to lysis and whole genome amplification (WGA) using a novel EquiPhi29TM DNA polymerase [100, 101], followed by Illumina sequencing, assembly, and annotation (Co-I Martinez-Garcia). With this unique dataset, we will determine the diversity and genomic composition of sediment viruses released from active microbial hosts under conditions where AOM is catalyzed by ANME alone or in syntrophy with a bacterial partner, or under CH₄ limitation. The SVG sequenced from our incubation experiments will be combined with existing metaviromic data to identify viral proteins in our paired metaproteomes (with either BONCAT or protein-SIP). Co-I Hettich and others have previously analyzed viral proteins from environmental samples [102, 103], and preliminary screening of our sediment metaproteomes identified >100 putative viral proteins, including structural viral proteins (terminase, capsid proteins) and an AMG (metK), suggesting we will be able to simultaneously recover microbial proteins alongside viruses in our sediment incubations.

III.3.a Environmental scale: Tracking activity of AOM consortia and viral interactions in physical context using transparent sediment model matrices. Caltech materials science colleague Kathy Faber has developed methods for synthesizing mineral structures with defined pore structure and connectivity. Here, precise control of the orientation and patterning of crystal growth for creation of dendritic pores is accomplished using novel directional freeze-casting with a solution of a preceramic polymer [104]. These ceramic structures provide a combination of high flow through the main channels and a series of low-exchange, high-surface-area side chambers, whose specific dimensions and connectivity can be precisely controlled during the synthesis process (**Fig.7**). This synthetic system provides a unique, reproducible experimental matrix in which to empirically test and model the effects of the physical environment on the distribution of active AOM consortia, associated geochemical gradients, and new viral production. With this laboratory system, we hope to fill a critical experimental gap for developing a systems-level understanding of methane-saturated sediment ecosystems, providing a bridge between the complex, heterogeneous native lithified sediment environment (where pore structure and connectivity have been imaged by XRM or neutron imaging; see letter of support, O'Neill), and the matrix-free multi-species enrichments of AOM aggregates in the laboratory. In collaboration with Faber (see letter of support), we will experiment with this freeze-casting technique to template minerals with optical properties compatible with microscopy. Here we will use cryolite, a mineral used as a transparent soil matrix by Caltech postdoc Sharma [80]. When submerged, cryolite has a refractive index identical to that of water, rendering it optically transparent and compatible with fluorescence microscopy, enabling application of fluorescence indicator dyes (e.g. Thioflavin T and CTC) for non-destructive monitoring of redox active cells; SNARF dyes for ratiometric fluorescence measurement of extracellular pH; BODIPY-flavin for measurement of extracellular redox state; and azaBODIPY for measurement of extracellular ammonia concentrations [105–

109] and real-time visualization of microbial cells and consortia within the mineral matrix. The properties of cryolite are compatible with the freeze-casting method, and proof-of-principle tests have confirmed that the standard freeze-casting process is non-toxic to anaerobic microorganisms. Here we will synthesize cryolite coupons with varying pore structure and permeability and inoculate with our sediment-free AOM enrichment culture (III.2.a). These coupons will be incubated at Caltech and loaded in a sealed microscopy-compatible chamber (Leica SampLink) with methane for live cell imaging, tracking microbial growth,

Fig. 7 Feedbacks between AOM and the local microenvironment: integration of *in situ* imaging, reaction transport modeling, FBM/CMM modeling, and synthetic sediment systems. (A) Our previous work has generated data on the pore structures of native lithified sediments hosting AOM consortia using micro-CT and neutron scattering. Locations of AOM



consortia within the pore space have also been visualized using DNA stains and FISH. These datasets will inform and constrain integrated computational models (III.3.b) (B) wherein genomics-enabled flux balance metabolic models are integrated with reaction transport models to obtain mm-scale 3D models of AOM biomass distributions, pore structure, and geochemical gradients. Predictions generated from these models will be compared with synthetic sediment matrices (C) generated by a novel freeze-casting process that enable precise pore structure, controlled flow rates, and optical transparency. Results from these transparent sediment experiments will be used to update computational models and refine experiments with natural sediments. This integrated pipeline will help iteratively refine our understanding of AOM and associated community dynamics at the microscale.

activity, and local environmental conditions over time. Active experiments in SampLink chambers will also be transported to NCMIR for imaging and embedding as described (III.1.c). This novel setup will enable us to examine the effect of simulated sediment pore and permeability on cellular activity and geochemical gradients. Transparent matrix experiments with HPG will also be conducted (III.2.b). Results will be compared with predictions from reaction transport models (Co-I Meile; III.3.b) to understand the influence of the physical matrix on methane-fueled syntrophic consortia and associated activity of viruses.

III.3.b Bridging intra-consortia and environment with integrated FBM and reaction-transport models. To integrate our syntrophic consortia-focused data and modeling into a more comprehensive ecosystems-level framework, we are continuing to develop computational methods which combine cell-specific flux balance models (FBM) with environmental reaction transport simulations, specifically focused on understanding the feedbacks and controls on the distribution and activities of AOM consortia and associated community members in methane-saturated sediments. The current DOE collaboration between Co-I's Henry and Orphan has significantly improved our ability to construct flux balance models using the open-source ModelSEED pipeline implemented in KBase [110]. Notably, we improved our capacity to reconstruct pathways in archaea as well as the ability to characterize and quantitatively predict diverse microbial energy biosynthesis strategies, including sulfate and nitrogen respiration, methanogenesis, and archaeal methane oxidation [111]. We then applied the improved ModelSEED to construct models of hundreds of Archaea, ANME, and SRB genomes in KBase. We combined our ANME and SRB models into a community metabolic model (CMM) to predict mechanistically how these species will interact. These

CMMs [112] are powerful tools for data integration, as they provide a mechanistic framework of all reactions known to take place within each species in the system. Metabolite flux within the community is then constrained based on fundamental physical principles: mass balance within each species and the environment, thermodynamic feasibility, and simplified kinetics [112–114]. This model framework can be integrated with a range of data types using additional constraints and objective functions (e.g. metatranscriptomic and proteomic datasets), by favoring flux solutions that involve reactions with highly expressed genes [115] and integrating flux measurements of metabolites by constraining the overall metabolite uptake and excretion by the CMM.

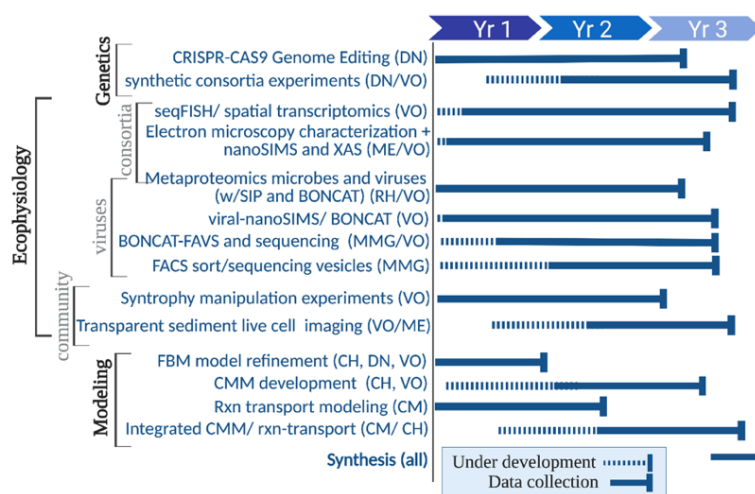
With this previous work, we are now poised to apply species and community models to make substantial new advancements. First, models will be applied to help identify all additional gene functions that are required to support ANME-style metabolism and the essential interactions with SRB in *Methanosarcina*. This will support the efforts of Co-I Nayak to produce an ANME-like mutant of *Methanosarcina* (see III.1). In turn, we expect these gene editing experiments will reveal new annotations and functions that will be integrated into our archaeal FBM and CMMs to improve accuracy and completeness. Similarly, insights from our models will inform physiological experiments with *Methanosarcina* mutants. This distinctive approach offers a highly targeted method to rapidly improve mechanistic understanding of ANME and associated interactions with SRB and other microbial species. Next, we will expand the scope of our CMMs from purely ANME-SRB interactions to *in silico* community-wide simulations with multiple ANME/ SRB lineages, distinct ANME ecotypes, methanogens, and other community members. These CMMs will produce balanced overall chemical reactions around each organism in the community, describing chemical activity scaled by biomass. Such overall reactions serve as critical inputs for the spatial dynamic modeling to be performed with Co-I Meile (see below). We will construct these expanded CMMs for each experimentally sampled microbiome system, integrating all data collected (e.g. metaproteomics, species abundance, environmental conditions, and species genomes) to predict overall flux profiles and individual species activities in each sample. All CMM outputs will serve as training sets to develop general neural network (NN) models for each species, which will enable rapid scalable computation of species chemical activity based on available nutrients and microbiome neighborhood (e.g. relative abundance of all co-localized species) [116].

These NN models will be used in our spatial dynamic simulations, facilitating the direct integration of 'omics-driven mechanistic insights into our reaction transport simulations (Co-I Meile; Fig.7) and capturing the key features of the physico-chemical environment. We have integrated 3D structural data of lithified methane-saturated sediments measured using XRM into our pore-scale Lattice Boltzmann models and we are now positioned to carry out pore-scale simulations of fluid flow and solute transport in the context of AOM consortia biomass distribution, where heterogeneous metabolic activities are impacted by, and dynamically transform, geochemical gradients. These models will be applied to quantify residence times and predict the distribution of substrates in transparent sediments and reaction products that affect microbial activity [62, 63, 117]. We will use concentration-dependent descriptions of uptake fluxes and refine our model by simulating the proposed transparent sediment experiments (III.3.a), for which imaging of chemical tracers (e.g. pH, redox) will provide unique chemical constraints on AOM-environment feedbacks at the microscale. We will then use our environmental modelling results in XRM-characterized natural settings and include the effect of viral cell lysis and the potential impact of virus transport [118–120] to identify potential spatial niches and favorable metabolic pathways for diverse AOM consortia and other community members, and we will compare them with our empirical ecophysiology data to identify similarities and differences and explore their underlying physiological reasons.

Our recent pore-scale reactive transport developments [Jung et al., in prep] allow for such direct integration of detailed descriptions of microbial metabolism as captured in FBMs/CCMs (subject to estimates of relationships between concentrations and upper limits of substrate uptake). To make such explorations computationally tractable, we will use reduced-complexity models such the above mentioned NN approximations and – if necessary – will employ pore network models [121, 122], which we can validate by comparison to our Lattice Boltzmann simulations.

Deliverables: At the heart of our cross-disciplinary project sit inter-Domain diverse syntrophies between environmental ANME archaea and bacteria that catalyze the globally important process of methane oxidation. Although their (meta)genomic context is well developed, there are several fundamental knowledge gaps about their physiology, mechanisms shaping syntrophic partner pairings, niche partitioning, interactions with other core microbial and viral ecosystem members, and resiliency to changing environmental conditions, which we will address here. Our proposed hypothesis-

driven, systems-level research on diverse AOM consortia in the context of the inherent complexity of associated biological and physico-chemical conditions in their local sedimentary environment is directly in line with the stated objectives of this FOA, which are to enhance understanding and predictive frameworks for dynamic microbial interactions in natural environments. The experimentally validated computational modeling framework we will advance is modular in its design, beginning at the consortia scale with core pair-wise syntrophic archaeal-bacterial interactions which drive methane oxidation, building out to community-level layers of the dominant microbial and viral interactions, and finally integrating physico-chemical processes and spatial context in the environment. Our integrative methodological approach will not only provide insights into the essential aspects of metabolic and ecological interactions of ANME-bacterial consortia, but may also uncover generalizable principles of anaerobic microbial ecosystems structure, with methodologies that are broadly applicable to other environments.



IV. Timeline, management, personnel. This three-year multidisciplinary project will be led through a synergistic collaboration between PIs from CIT, UGA, UCSD, UCB, ANL, ORNL, and UA. **PI Orphan** (CIT) will lead this team, building on her many years of experience studying the ecology of environmental methane-oxidizing consortia using single-cell resolved molecular and isotopic methods. She will serve as the project coordinator, responsible for overseeing project management, data sharing, and annual reporting to DOE. Her lab will lead the proposed experiments with AOM sediment communities and single cell ecophysiological experiments. **PI Nayak** (UCB) pioneered the development of CRISPR gene editing in *Methanosarcina*. She will lead heterologous expression experiments with ANME genes, work with Orphan to build synthetic consortia, and advise Henry with refining annotations and FBM models of syntrophic AOM. **PI Martinez-Garcia** (UA) is a leading expert in using flow cytometry to sort and sequence single viruses from the environment. He will be responsible for sorting and sequencing BONCAT-labelled viruses and vesicles from sediment experiments and will oversee genomic data collection and analysis. **PI Meile** (UGA) will lead reaction-transport model development, working closely with Orphan, Ellisman, and Henry to develop an integrated methane-based community metabolic model (CMM) in the spatial context of the sediment environment. **PI Henry** (ANL) will lead the development of CMM, refine FBM models for individual genomes, and assist with interpretations of *in silico* FBM/CMM model predictions that will be empirically tested in the lab. He will also work with the KBase team to integrate new workflows and data from this project (letter Arkin). **PI Ellisman** (UCSD) is the Director of the National Center for Microbial Imaging Research. He will work with Orphan on live cell imaging and will conduct EM analyses on consortia, focused on structural characterization of the ECM. **PI Hettich** (ORNL) is the head of the Bioanalytical Mass Spectrometry Group, with over three decades of experience in high-performance biological mass spectrometry. He will be responsible for metaproteomics of sediment microorganisms and viruses using protein-SIP and BONCAT.

Appendix 3. Bibliography & References Cited

(references in bold are associated with the PI's)

1. Reeburgh WS. Oceanic Methane Biogeochemistry. *Chem Rev* 2007; **107**: 486–513.
2. Su G, Zopfi J, Yao H, Steinle L, Niemann H, Lehmann MF. Manganese/iron-supported sulfate-dependent anaerobic oxidation of methane by archaea in lake sediments. *Limnol Oceanogr* 2020; **65**: 863–875.
3. Knittel K, Boetius A. Anaerobic Oxidation of Methane: Progress with an Unknown Process. *Annu Rev Microbiol* 2009; **63**: 311–334.
4. Reeburgh WS, Heggie DT. Microbial methane consumption reactions and their effect on methane distributions in freshwater and marine environments. *Limnol Oceanogr* 1977; **22**: 1–9.
5. Hoehler TM, Alperin MJ, Albert DB, Martens CS. Field and laboratory studies of methane oxidation in an anoxic marine sediment: Evidence for a methanogen-sulfate reducer consortium. *Global Biogeochem Cycles* 1994; **8**: 451–463.
6. Sørensen KB, Finster K, Ramsing NB. Thermodynamic and kinetic requirements in anaerobic methane oxidizing consortia exclude hydrogen, acetate, and methanol as possible electron shuttles. *Microb Ecol* 2001; **42**: 1–10.
7. Alperin MJ, Hoehler TM. Anaerobic methane oxidation by archaea/sulfate-reducing bacteria aggregates: 1. Thermodynamic and physical constraints. *Am J Sci* 2009; **309**: 869–957.
8. Hallam SJ, Putnam N, Preston CM, Detter JC, Rokhsar D, Richardson PM, et al. Reverse methanogenesis: testing the hypothesis with environmental genomics. *Science* 2004; **305**: 1457–1462.
9. Meyerdierks A, Kube M, Kostadinov I, Teeling H, Glöckner FO, Reinhardt R, et al. Metagenome and mRNA expression analyses of anaerobic methanotrophic archaea of the ANME-1 group. *Environ Microbiol* 2010; **12**: 422–439.
10. **Pernthaler A, Dekas AE, Brown CT, Goffredi SK, Embaye T, Orphan VJ. Diverse syntrophic partnerships from-deep-sea methane vents revealed by direct cell capture and metagenomics. *Proc Natl Acad Sci USA* 2008; **105**: 7052–7057.**
11. Haroon MF, Hu S, Shi Y, Imelfort M, Keller J, Hugenholtz P, et al. Anaerobic oxidation of methane coupled to nitrate reduction in a novel archaeal lineage. *Nature* 2013; **500**: 567–570.
12. Wang FP, Zhang Y, Chen Y, He Y, Qi J, Hinrichs KU, et al. Methanotrophic archaea possessing diverging methane-oxidizing and electron-transporting pathways. *ISME J* 2014; **8**: 1069–78.
13. Thauer RK. Anaerobic oxidation of methane with sulfate: on the reversibility of the reactions that are catalyzed by enzymes also involved in methanogenesis from CO₂. *Curr Opin Microbiol* 2011; **14**: 292–299.
14. **Chadwick GL, Skennerton CT, Laso-Pérez R, Leu AO, Speth DR, Yu H, et al. Comparative genomics reveals electron transfer and syntrophic mechanisms differentiating methanotrophic and methanogenic archaea. *PLOS Biology* 2022; **20**: e3001508.**

15. Leu AO, Cai C, McIlroy SJ, Southam G, Orphan VJ, Zhiguo Y, et al. Anaerobic methane oxidation coupled to manganese reduction by members of the Methanoperedenaceae. *ISME J* 2020; 14: 1030–1041.
16. McGlynn SE, Chadwick GL, Kempes CP, Orphan VJ. Single cell activity reveals direct electron transfer in methanotrophic consortia. *Nature* 2015; 526: 531–535.
17. Wegener G, Krukenberg V, Riedel D, Tegetmeyer HE, Boetius A. Intercellular wiring enables electron transfer between methanotrophic archaea and bacteria. *Nature* 2015; 526: 587–590.
18. Timmers PHA, Welte CU, Koehorst JJ, Plugge CM, Jetten MSM, Stams AJM. Reverse Methanogenesis and Respiration in Methanotrophic Archaea. *Archaea* 2017; 2017: e1654237.
19. Hatzenpichler R, Connon SA, Goudeau D, Malmstrom RR, Woyke T, Orphan VJ. Visualizing in situ translational activity for identifying and sorting slow-growing archaeal-bacterial consortia. *Proc Natl Acad Sci USA* 2016; 113: E4069-78.
20. Yu H, Speth DR, Connon SA, Goudeau D, Malmstrom RR, Woyke T, et al. Community structure and microbial associations in sediment-free methanotrophic enrichment cultures from a marine methane seep. 2022, in review *Appl. Environ. Microbiol.*
21. Krukenberg V, Harding K, Richter M, Glockner FO, Gruber-Vodicka HR, Adam B, et al. Candidatus Desulfotomaculum auxilii, a hydrogenotrophic sulfate-reducing bacterium involved in the thermophilic anaerobic oxidation of methane. *Environ Microbiol* 2016; 18: 3073–3091.
22. Skennerton CT, Chourey K, Iyer R, Hettich RL, Tyson GW, Orphan VJ. Methane-Fueled Syntrophy through Extracellular Electron Transfer: Uncovering the Genomic Traits Conserved within Diverse Bacterial Partners of Anaerobic Methanotrophic Archaea. *Mbio* 2017; 8: e00530-17.
23. Krukenberg V, Riedel D, Gruber-Vodicka HR, Buttigieg PL, Tegetmeyer HE, Boetius A, et al. Gene expression and ultrastructure of meso- and thermophilic methanotrophic consortia. *Environ Microbiol* 2018; 20: 1651–1666.
24. Metcalfe KS, Murali R, Mullin SW, Connon SA, Orphan VJ. Experimentally-validated correlation analysis reveals new anaerobic methane oxidation partnerships with consortium-level heterogeneity in diazotrophy. *ISME J* 2021; 15: 377–396.
25. Kashtan N, Roggensack SE, Rodrigue S, Thompson JW, Biller SJ, Coe A, et al. Single-Cell Genomics Reveals Hundreds of Coexisting Subpopulations in Wild *Prochlorococcus*. *Science* 2014; 344: 416–420.
26. Crits-Christoph A, Olm MR, Diamond S, Bouma-Gregson K, Banfield JF. Soil bacterial populations are shaped by recombination and gene-specific selection across a grassland meadow. *ISME J* 2020; 14: 1834–1846.
27. Chase AB, Arevalo P, Brodie EL, Polz MF, Karaoz U, Martiny JBH. Maintenance of Sympatric and Allopatric Populations in Free-Living Terrestrial Bacteria. *mBio* 2019; 10: e02361-19.

28. Wegener G, Krukenberg V, Ruff SE, Kellermann MY, Knittel K. Metabolic Capabilities of Microorganisms Involved in and Associated with the Anaerobic Oxidation of Methane. *Front Microbiol* 2016; **7**.
29. Scheller S, Yu H, Chadwick GL, McGlynn SE, Orphan VJ. Artificial electron acceptors decouple archaeal methane oxidation from sulfate reduction. *Science* 2016; **351**: 703–707.
30. Yu H, Skennerton CT, Chadwick GL, Leu AO, Aoki M, Tyson GW, et al. Sulfate differentially stimulates but is not respired by diverse anaerobic methanotrophic archaea. *ISME J* 2022; **16**: 168–177.
31. Lovley DR. Happy together: microbial communities that hook up to swap electrons. *ISME J* 2017; **11**: 327–336.
32. Rotaru A-E, Yee MO, Musat F. Microbes trading electricity in consortia of environmental and biotechnological significance. *Curr Opin Biotechnol* 2021; **67**: 119–129.
33. Milucka J, Ferdelman TG, Polerecky L, Franzke D, Wegener G, Schmid M, et al. Zero-valent sulphur is a key intermediate in marine methane oxidation. *Nature* 2012; **491**: 541–546.
34. Jiménez Otero F, Chadwick GL, Yates MD, Mickol RL, Saunders SH, Glaven SM, et al. Evidence of a Streamlined Extracellular Electron Transfer Pathway from Biofilm Structure, Metabolic Stratification, and Long-Range Electron Transfer Parameters. *Appl Environ Microbiol* 2021; **87**: e00706-21.
35. Nayak DD, Metcalf WW. Cas9-mediated genome editing in the methanogenic archaeon *Methanosarcina acetivorans*. *Proc Natl Acad Sci USA* 2017; **114**: 2976–2981.
36. Orphan VJ, House CH, Hinrichs K-U, McKeegan KD, DeLong EF. Multiple archaeal groups mediate methane oxidation in anoxic cold seep sediments. *Proc Natl Acad Sci USA* 2002; **99**: 7663–7668.
37. Boetius A, Ravensschlag K, Schubert CJ, Rickert D, Widdel F, Gieseke A, et al. A marine microbial consortium apparently mediating anaerobic oxidation of methane. *Nature* 2000; **407**: 623–626.
38. Orphan VJ, House CH, Hinrichs K-U, McKeegan KD, DeLong EF. Methane-Consuming Archaea Revealed by Directly Coupled Isotopic and Phylogenetic Analysis. *Science* 2001; **293**: 484–487.
39. Knittel K, Lösekann T, Boetius A, Kort R, Amann R. Diversity and Distribution of Methanotrophic Archaea at Cold Seeps. *Appl Environ Microbiol* 2005; **71**: 467–479.
40. Laso-Pérez R, Krukenberg V, Musat F, Wegener G. Establishing anaerobic hydrocarbon-degrading enrichment cultures of microorganisms under strictly anoxic conditions. *Nat Protoc* 2018; **13**: 1310–1330.
41. Gründger F, Carrier V, Svenning MM, Panieri G, Vonnahme TR, Klasek S, et al. Methane-fuelled biofilms predominantly composed of methanotrophic ANME-1 in Arctic gas hydrate-related sediments. *Sci Rep* 2019; **9**: 9725.

42. Trembath-Reichert E, Case DH, Orphan VJ. Characterization of microbial associations with methanotrophic archaea and sulfate-reducing bacteria through statistical comparison of nested Magneto-FISH enrichments. *PeerJ* 2016; 4: e1913.
43. House CH, Orphan VJ, Turk KA, Thomas B, Pernthaler A, Vrentas JM, et al. Extensive carbon isotopic heterogeneity among methane seep microbiota. *Environ Microbiol* 2009; 11: 2207–2215.
44. Ruff SE, Biddle JF, Teske AP, Knittel K, Boetius A, Ramette A. Global dispersion and local diversification of the methane seep microbiome. *Proc Natl Acad Sci USA* 2015; 112: 4015–4020.
45. Kevorkian RT, Sipes K, Winstead R, Paul R, Lloyd KG. Cryptic Methane-Cycling by Methanogens During Multi-Year Incubation of Estuarine Sediment. *Front Microbiol* 2022; 13.
46. Beulig F, Røy H, McGlynn SE, Jørgensen BB. Cryptic CH₄ cycling in the sulfate–methane transition of marine sediments apparently mediated by ANME-1 archaea. *ISME J* 2019; 13: 250–262.
47. Li H, Yang Q, Zhou H. Niche Differentiation of Sulfate- and Iron-Dependent Anaerobic Methane Oxidation and Methylophilic Methanogenesis in Deep Sea Methane Seeps. *Front Microbiol* 2020; 11.
48. Emerson JB, Roux S, Brum JR, Bolduc B, Woodcroft BJ, Jang HB, et al. Host-linked soil viral ecology along a permafrost thaw gradient. *Nat Microbiol* 2018; 3: 870–880.
49. Lee S, Sieradzki ET, Nicolas AM, Walker RL, Firestone MK, Hazard C, et al. Methane-derived carbon flows into host–virus networks at different trophic levels in soil. *Proc Natl Acad Sci USA* 2021; 118: e2105124118.
50. Chen L-X, Méheust R, Crits-Christoph A, McMahon KD, Nelson TC, Slater GF, et al. Large freshwater phages with the potential to augment aerobic methane oxidation. *Nat Microbiol* 2020; 5: 1504–1515.
51. Paul BG, Bagby SC, Czornyj E, Arambula D, Handa S, Sczyrba A, et al. Targeted diversity generation by intraterrestrial archaea and archaeal viruses. *Nat Commun* 2015; 6: 7585.
52. Li Z, Pan D, Wei G, Pi W, Zhang C, Wang J-H, et al. Deep sea sediments associated with cold seeps are a subsurface reservoir of viral diversity. *ISME J* 2021; 15: 2366–2378.
53. Bryson SJ, Thurber AR, Correa AMS, Orphan VJ, Thurber RV. A novel sister clade to the enterobacteria microviruses (family Microviridae) identified in methane seep sediments. *Environ Microbiol* 2015; 17: 3708–3721.
54. Zimmerman AE, Howard-Varona C, Needham DM, John SG, Worden AZ, Sullivan MB, et al. Metabolic and biogeochemical consequences of viral infection in aquatic ecosystems. *Nat Rev Microbiol* 2020; 18: 21–34.
55. Pasulka AL, Thametrakoln K, Kopf SH, Guan Y, Poulos B, Moradian A, et al. Interrogating marine virus-host interactions and elemental transfer with BONCAT and nanoSIMS-based methods. *Environ Microbiol* 2018; 20: 671–692.

56. McGlynn SE, Chadwick GL, O'Neill A, Mackey M, Thor A, Deerinck TJ, et al. Subgroup Characteristics of Marine Methane-Oxidizing ANME-2 Archaea and Their Syntrophic Partners as Revealed by Integrated Multimodal Analytical Microscopy. *Appl Environ Microbiol* 2018; **84**: e00399-18.
57. Hatzenpichler R, Krukenberg V, Spietz RL, Jay ZJ. Next-generation physiology approaches to study microbiome function at single cell level. *Nat Rev Microbiol* 2020; **18**: 241–256.
58. Lubeck E, Coskun AF, Zhiyentayev T, Ahmad M, Cai L. Single-cell in situ RNA profiling by sequential hybridization. *Nature Methods* 2014; **11**: 360–1.
59. Eng C-HL, Lawson M, Zhu Q, Dries R, Koulina N, Takei Y, et al. Transcriptome-scale super-resolved imaging in tissues by RNA seqFISH+. *Nature* 2019; **568**: 235–239.
60. Choi HMT, Schwarzkopf M, Fornace ME, Acharya A, Artavanis G, Stegmaier J, et al. Third-generation in situ hybridization chain reaction: multiplexed, quantitative, sensitive, versatile, robust. *Development (Cambridge, England)* 2018; **145**: dev165753.
61. Orcutt B, Meile C. Constraints on mechanisms and rates of anaerobic oxidation of methane by microbial consortia: process-based modeling of ANME-2 archaea and sulfate reducing bacteria interactions. *Biogeosciences* 2008; **5**: 1587–1599.
62. He X, Chadwick G, Kempes C, Shi Y, McGlynn S, Orphan V, et al. Microbial interactions in the anaerobic oxidation of methane: model simulations constrained by process rates and activity patterns. *Environ Microbiol* 2019; **21**: 631–647.
63. He X, Chadwick GL, Kempes CP, Orphan VJ, Meile C. Controls on Interspecies Electron Transport and Size Limitation of Anaerobically Methane-Oxidizing Microbial Consortia. *mBio* 2021; **12**: e03620-20.
64. He X, Chadwick G, Jiménez Otero F, Orphan V, Meile C. Spatially Resolved Electron Transport through Anode-Respiring *Geobacter sulfurreducens* Biofilms: Controls and Constraints. *ChemElectroChem* 2021; **8**: 1747–1758.
65. Toyofuku M, Nomura N, Eberl L. Types and origins of bacterial membrane vesicles. *Nat Rev Microbiol* 2019; **17**: 13–24.
66. Kulp A, Kuehn MJ. Biological Functions and Biogenesis of Secreted Bacterial Outer Membrane Vesicles. *Annu Rev Microbiol* 2010; **64**: 163–184.
67. Tsatsaronis JA, Franch-Arroyo S, Resch U, Charpentier E. Extracellular Vesicle RNA: A Universal Mediator of Microbial Communication? *Trends Microbiol* 2018; **26**: 401–410.
68. McGlynn SE, Perkins G, Sim MS, Mackey M, Deerinck TJ, Thor A, et al. A Cristae-Like Microcompartment in *Desulfobacterota*. 2022, submitted.
69. Nayak DD, Metcalf WW. Chapter Thirteen - Genetic techniques for studies of methyl-coenzyme M reductase from *Methanosarcina acetivorans* C2A. In: Armstrong F (ed). *Methods in Enzymology*. 2018. Academic Press, pp 325–347.

70. Badalamenti JP, Summers ZM, Chan CH, Gralnick JA, Bond DR. Isolation and Genomic Characterization of ‘Desulfuromonas soudanensis WTL’, a Metal- and Electrode-Respiring Bacterium from Anoxic Deep Subsurface Brine. *Front Microbiol* 2016; **7**.
71. Summers ZM, Fogarty HE, Leang C, Franks AE, Malvankar NS, Lovley DR. Direct exchange of electrons within aggregates of an evolved syntrophic coculture of anaerobic bacteria. *Science* 2010; **330**: 1413–1415.
72. Rotaru A-E, Shrestha PM, Liu F, Markovaitė B, Chen S, Nevin KP, et al. Direct Interspecies Electron Transfer between *Geobacter metallireducens* and *Methanosarcina barkeri*. *Appl Environ Microbiol* 2014; **80**: 4599–4605.
73. Chan CH, Levar CE, Zacharoff L, Badalamenti JP, Bond DR. Scarless Genome Editing and Stable Inducible Expression Vectors for *Geobacter sulfurreducens*. *Appl Environ Microbiol* 2015; **81**: 7178–7186.
74. Dar D, Dar N, Cai L, Newman DK. Spatial transcriptomics of planktonic and sessile bacterial populations at single-cell resolution. *Science* 2021; **373**: eabi4882.
75. Wrede C, Kokoschka S, Dreier A, Heller C, Reitner J, Hoppert M. Deposition of Biogenic Iron Minerals in a Methane Oxidizing Microbial Mat. *Archaea* 2013; **2013**: e102972.
76. Felz S, Kleikamp H, Zlopasa J, van Loosdrecht MCM, Lin Y. Impact of metal ions on structural EPS hydrogels from aerobic granular sludge. *Biofilm* 2020; **2**: 100011.
77. Neu TR, Swerhone GDW, Lawrence JRY 2001. Assessment of lectin-binding analysis for in situ detection of glycoconjugates in biofilm systems. *Microbiology* 2001; **147**: 299–313.
78. Zhang RY, Neu TR, Bellenberg S, Kuhlicke U, Sand W, Vera M. Use of lectins to in situ visualize glycoconjugates of extracellular polymeric substances in acidophilic archaeal biofilms. *Microbial Biotechnology* 2015; **8**: 448–461.
79. Böck D, Medeiros JM, Tsao H-F, Penz T, Weiss GL, Aistleitner K, et al. In situ architecture, function, and evolution of a contractile injection system. *Science* 2017; **357**: 713–717.
80. Sharma K, Palatinszky M, Nikolov G, Berry D, Shank EA. Transparent soil microcosms for live-cell imaging and non-destructive stable isotope probing of soil microorganisms. *eLife* 2020; **9**: e56275.
81. Sachsenberg T, Herbst F-A, Taubert M, Kermer R, Jehmlich N, von Bergen M, et al. MetaProSIP: Automated Inference of Stable Isotope Incorporation Rates in Proteins for Functional Metaproteomics. *J Proteome Res* 2015; **14**: 619–627.
82. Li Z, Yao Q, Guo X, Crits-Christoph A, Mayes MA, IV WJH, et al. Genome-Resolved Proteomic Stable Isotope Probing of Soil Microbial Communities Using ¹³CO₂ and ¹³C-Methanol. *Front Microbiol* 2019; **10**.
83. Kieft B, Li Z, Bryson S, Hettich RL, Pan C, Mayali X, et al. Phytoplankton exudates and lysates support distinct microbial consortia with specialized metabolic and ecophysiological traits. *Proc Natl Acad Sci USA* 2021; **118**: e2101178118.

84. Hungate BA, Mau RL, Schwartz E, Caporaso JG, Dijkstra P, van Gestel N, et al. Quantitative Microbial Ecology through Stable Isotope Probing. *Appl Environ Microbiol* 2015; **81**: 7570–7581.
85. Ireland TR. SIMS measurement of stable isotopes. *Handbook of stable isotope analytical technique*. 2004. pp 652–691.
86. Slodzian G, Daigne B, Girard F, Boust F, Hillion F. Scanning secondary ion analytical microscopy with parallel detection. *Biology of the Cell* 1992; **74**: 43–50.
87. Orphan VJ, Hinrichs K-U, Ussler W, Paull CK, Taylor LT, Sylva SP, et al. Comparative Analysis of Methane-Oxidizing Archaea and Sulfate-Reducing Bacteria in Anoxic Marine Sediments. *Appl Environ Microbiol* 2001; **67**: 1922–1934.
88. Orphan VJ. Methods for unveiling cryptic microbial partnerships in nature. *Current Opinion in Microbiology* 2009; **12**: 231–237.
89. Musat N, Musat F, Weber PK, Pett-Ridge J. Tracking microbial interactions with NanoSIMS. *Curr Opin Biotechnol* 2016; **41**: 114–121.
90. Trembath-Reichert E, Morono Y, Ijiri A, Hoshino T, Dawson KS, Inagaki F, et al. Methyl-compound use and slow growth characterize microbial life in 2-km-deep seafloor coal and shale beds. *Proc Natl Acad Sci USA* 2017; **114**: E9206–e9215.
91. Dawson KS, Scheller S, Dillon JG, Orphan VJ. Stable Isotope Phenotyping via Cluster Analysis of NanoSIMS Data As a Method for Characterizing Distinct Microbial Ecophysiology and Sulfur-Cycling in the Environment. *Front Microbiol* 2016; **7**.
92. Fike DA, Houghton JL, Moore SE, Gilhooly WP, Dawson KS, Druschel GK, et al. Spatially resolved capture of hydrogen sulfide from the water column and sedimentary pore waters for abundance and stable isotopic analysis. *Mar Chem* 2017; **197**: 26–37.
93. Martinez-Hernandez F, Fornas O, Lluesma Gomez M, Bolduc B, de la Cruz Pena MJ, Martinez JM, et al. Single-virus genomics reveals hidden cosmopolitan and abundant viruses. *Nat Commun* 2017; **8**: 15892.
94. de la Cruz Pena MJ, Martinez-Hernandez F, Garcia-Heredia I, Lluesma Gomez M, Fornas O, Martinez-Garcia M. Deciphering the Human Virome with Single-Virus Genomics and Metagenomics. *Viruses* 2018; **10**: v10030113.
95. Martinez-Hernandez F, Diop A, Garcia-Heredia I, Bobay L-M, Martinez-Garcia M. Unexpected myriad of co-occurring viral strains and species in one of the most abundant and microdiverse viruses on Earth. *ISME J* 2022; **16**: 1025–1035.
96. Martínez Martínez J, Martinez-Hernandez F, Martinez-Garcia M. Single-virus genomics and beyond. *Nat Rev Microbiol* 2020; **18**: 705–716.
97. Schatz D, Vardi A. Extracellular vesicles — new players in cell–cell communication in aquatic environments. *Curr Opin Microbiol* 2018; **43**: 148–154.

98. Biller SJ, Lundeen RA, Hmelo LR, Becker KW, Arellano AA, Dooley K, et al. Prochlorococcus extracellular vesicles: molecular composition and adsorption to diverse microbes. *Environ Microbiol* 2022; **24**: 420–435.
99. Schwechheimer C, Kuehn MJ. Outer-membrane vesicles from Gram-negative bacteria: biogenesis and functions. *Nat Rev Microbiol* 2015; **13**: 605–619.
100. Stepanauskas R, Fergusson EA, Brown J, Poulton NJ, Tupper B, Labonte JM, et al. Improved genome recovery and integrated cell-size analyses of individual uncultured microbial cells and viral particles. *Nat Commun* 2017; **8**: 84.
- 101. Garcia-Heredia I, Bhattacharjee AS, Fornas O, Gomez ML, Martínez JM, Martinez-Garcia M. Benchmarking of single-virus genomics: a new tool for uncovering the virosphere. *Environ Microbiol* 2021; **23**: 1584–1593.**
- 102. Belnap CP, Pan C, Denev VJ, Samatova NF, Hettich RL, Banfield JF. Quantitative proteomic analyses of the response of acidophilic microbial communities to different pH conditions. *ISME J* 2011; **5**: 1152–1161.**
103. Brum JR, Ignacio-Espinoza JC, Kim E-H, Trubl G, Jones RM, Roux S, et al. Illuminating structural proteins in viral “dark matter” with metaproteomics. *Proc Natl Acad Sci USA* 2016; **113**: 2436–2441.
104. Naviroj M, Voorhees PW, Faber KT. Suspension- and solution-based freeze casting for porous ceramics. *J Mater Res* 2017; **32**: 3372–3382.
105. Prindle A, Liu J, Asally M, Ly S, Garcia-Ojalvo J, Süel GM. Ion channels enable electrical communication in bacterial communities. *Nature* 2015; **527**: 59–63.
106. Rodriguez GG, Phipps D, Ishiguro K, Ridgway HF. Use of a fluorescent redox probe for direct visualization of actively respiring bacteria. *Appl Environ Microbiol* 1992; **58**: 1801–1808.
107. Hunter RC, Beveridge TJ. Application of a pH-Sensitive Fluoroprobe (C-SNARF-4) for pH Microenvironment Analysis in *Pseudomonas aeruginosa* Biofilms. *Appl Environ Microbiol* 2005; **71**: 2501–2510.
108. Yamada Y, Tomiyama Y, Morita A, Ikekita M, Aoki S. BODIPY-Based Fluorescent Redox Potential Sensors that Utilize Reversible Redox Properties of Flavin. *ChemBioChem* 2008; **9**: 853–856.
109. Strobl M, Walcher A, Mayr T, Klimant I, Borisov SM. Trace Ammonia Sensors Based on Fluorescent Near-Infrared-Emitting aza-BODIPY Dyes. *Anal Chem* 2017; **89**: 2859–2865.
110. Arkin AP, Cottingham RW, Henry CS, Harris NL, Stevens RL, Maslov S, et al. KBase: The United States Department of Energy Systems Biology Knowledgebase. *Nat Biotechnol* 2018; **36**: 566–569.
111. Faria JP, Liu F, Edirisinghe JN, Gupta N, Weisenhorn P, Sakkaff Z, et al. ModelSEED 2: High-throughput genome scale metabolic model reconstruction with enhanced Energy Biosynthesis Pathway Prediction. *bioRxiv*, 2022.

112. Henry CS, Bernstein HC, Weisenhorn P, Taylor RC, Lee JY, Zucker J, et al. Microbial Community Metabolic Modeling: A Community Data-Driven Network Reconstruction. *J Cell Physiol* 2016; **231**: 2339–2345.
113. Henry CS, Broadbelt LJ, Hatzimanikatis V. Thermodynamics-Based Metabolic Flux Analysis. *Biophys J* 2007; **92**: 1792–1805.
114. Chan SHJ, Simons MN, Maranas CD. SteadyCom: Predicting microbial abundances while ensuring community stability. *PLoS Comput Biol* 2017; **13**: e1005539.
115. Kim MK, Lun DS. Methods for integration of transcriptomic data in genome-scale metabolic models. *Comput Struct Biotechnol J* 2014; **11**: 59–65.
116. Wang S, Fan K, Luo N, Cao Y, Wu F, Zhang C, et al. Massive computational acceleration by using neural networks to emulate mechanism-based biological models. *Nat Commun* 2019; **10**: 4354.
117. Jung H, Meile C. Upscaling of microbially driven first-order reactions in heterogeneous porous media. *J Contam Hydrol* 2019.
118. Schijven JF, Hassanizadeh SM. Removal of Viruses by Soil Passage: Overview of Modeling, Processes, and Parameters. *Crit Rev Environ Sci Technol* 2000; **30**: 49–127.
119. Samari Kermani M, Jafari S, Rahn timer M, Raoof A. Direct pore scale numerical simulation of colloid transport and retention. Part I: Fluid flow velocity, colloid size, and pore structure effects. *Adv Water Res* 2020; **144**: 103694.
120. Molnar IL, Johnson WP, Gerhard JI, Willson CS, O’Carroll DM. Predicting colloid transport through saturated porous media: A critical review. *Water Resources Research* 2015; **51**: 6804–6845.
121. Gostick J, Aghighi M, Hinebaugh J, Tranter T, Hoeh MA, Day H, et al. OpenPNM: A Pore Network Modeling Package. *Comput Sci Eng* 2016; **18**: 60–74.
122. Varloteaux C, Békri S, Adler PM. Pore network modelling to determine the transport properties in presence of a reactive fluid: From pore to reservoir scale. *Adv Water Res* 2013; **53**: 87–100.